Geophysical Research Letters

RESEARCH LETTER
10.1029/2025GL114672

Characterizing the Interannual Variability of North Atlantic Subpolar Overturning

Yao Fu[1,2], M. Susan Lozier[1], Amy Bower[3], Kristin Burmeister[4], Tiago Carrilho Biló[5], Frédéric Cyr[6,7], Stuart A. Cunningham[4], Brad deYoung[8], Ahmad Fehmi Dilmahamod[9], M. Femke de Jong[10], Nora Fried[10,11], N. Penny Holliday[12], Neil J. Fraser[4], William E. Johns[13], Feili Li[14], Johannes Karstensen[9], Robert S. Pickart[3], Fiammetta Straneo[15], and Igor Yashayaev[16]

[1]School of Earth and Atmospheric Sciences, Georgia Institute of Technology, Atlanta, GA, USA, [2]College of Marine Science, University of South Florida, St. Peterburg, FL, USA, [3]Woods Hole Oceanographic Institution, Woods Hole, MA, USA, [4]Scottish Association for Marine Science, Oban, UK, [5]School of Marine Sciences, Climate Change Institute, University of Maine, Orono, ME, USA, [6]Northwest Atlantic Fisheries Centre, St. John's, NL, Canada, [7]Now at Centre for Fisheries and Ecosystem Research, Fisheries and Marine Institute of Memorial University, St. John's, NL, Canada, [8]Department of Physics and Physical Oceanography, Memorial University, St. John's, NL, Canada, [9]GEOMAR Helmholtz Centre for Ocean Research Kiel, Kiel, Germany, [10]Department of Ocean Systems, Royal Netherlands Institute for Sea Research NIOZ, Texel, The Netherlands, [11]Department of Geosciences, Institute of Landscape Ecology, University of Münster, Münster, Germany, [12]National Oceanography Centre, Southampton, UK, [13]Rosenstiel School of Marine, Atmospheric, and Earth Science, University of Miami, Miami, FL, USA, [14]State Key Laboratory of Marine Environmental Science & College of Ocean and Earth Sciences, Xiamen University, Xiamen, China, [15]Harvard University, Cambridge, MA, USA, [16]Bedford Institute of Oceanography, Dartmouth, NS, Canada

Key Points:

- The 8-year (2014–2022) Overturning in the Subpolar North Atlantic Program (OSNAP) time series of the Meridional Overturning Circulation (MOC) and meridional heat and freshwater transports are presented
- Individual boundary currents in the subpolar basins are accountable for up to 30% of MOC interannual variability
- Surface transformation across OSNAP East explains just 38% of MOC interannual variability; across OSNAP West it explains 27%

Supporting Information:

Supporting Information may be found in the online version of this article.

Correspondence to:

Y. Fu and M. S. Lozier,
yaofu@usf.edu;
susan.lozier@gatech.edu

Citation:

Fu, Y., Lozier, M. S., Bower, A., Burmeister, K., Carrilho Biló, T., Cyr, F., et al. (2025). Characterizing the interannual variability of North Atlantic subpolar overturning. *Geophysical Research Letters*, *52*, e2025GL114672. https://doi.org/10.1029/2025GL114672

Received 13 JAN 2025
Accepted 31 AUG 2025

Author Contributions:

Conceptualization: Yao Fu, M. Susan Lozier, William E. Johns
Data curation: Yao Fu, Kristin Burmeister, Tiago Carrilho Biló, Frédéric Cyr, Ahmad Fehmi Dilmahamod, Nora Fried, Neil J. Fraser, Igor Yashayaev
Formal analysis: Yao Fu
Funding acquisition: M. Susan Lozier, Amy Bower, Frédéric Cyr, Stuart A. Cunningham, Brad deYoung, M. Femke de Jong, N. Penny Holliday, William E. Johns, Johannes Karstensen, Robert S. Pickart, Fiammetta Straneo, Igor Yashayaev

Abstract Variability of the Atlantic Meridional Overturning Circulation (MOC) has drawn extensive attention due to its impact on the global redistribution of heat and freshwater. Here we present the latest time series (2014–2022) of the Overturning in the Subpolar North Atlantic Program and characterize MOC interannual variability. We find that any single boundary current captures ∼30% of subpolar MOC interannual variability. However, to fully resolve MOC variability, a wide swath across the eastern subpolar basin is needed; in the Labrador Sea both boundaries are needed. Through a volume budget analysis for the subpolar basins' lower limbs, we estimate the magnitude of unresolved processes (e.g., diapycnal mixing) required to close the mean budget (∼2 Sv). We find that in the eastern subpolar basin surface-forced transformation variability is linked to lower limb volume variability, which translates to MOC changes within the same year. In contrast, this linkage is weak in the Labrador Sea.

Plain Language Summary The Atlantic Meridional Overturning Circulation (AMOC) is important for the global climate due to its role in redistributing heat, freshwater, and dissolved gases over broad spatial scales. Through continuous observations, we now have an 8-year (2014–2022) time series of volume, heat and freshwater transports in the subpolar North Atlantic (∼60°N). Using these data, our analysis focuses on characterizing the interannual variability of the AMOC. We first investigated the importance of boundary currents and found that any single boundary current can account for up to ∼30% of the total AMOC interannual variability. Using a number of data sets, we then quantified the relationship between the water mass formation through surface cooling and freshening, the storage of water masses in ocean basins, and the AMOC on interannual timescales. We find an expected relationship in the eastern subpolar basin (between Greenland and the UK), where formation leads to increased basin storage, which further results in enhanced AMOC.

1. Introduction

As a key component of Earth's climate system, the Atlantic Meridional Overturning Circulation (MOC) plays a crucial role in redistributing heat, freshwater, nutrients, oxygen, and carbon globally. MOC variability, therefore, has profound implications for the global climate, marine ecosystems, regional weather, and sea level (Collins et al., 2019). The MOC consists of a northward-flowing upper limb and southward-flowing lower limb. As the warm and saline upper limb waters move northward, they gradually lose heat and mix with surrounding waters from the subpolar North Atlantic (SPNA) to the Arctic, forming the colder and fresher lower limb waters (Årthun et al., 2023; Weijer et al., 2022). The SPNA is a key region where this transformation occurs (Figure 1a).

Methodology: Yao Fu, Feili Li
Project administration: M. Susan Lozier
Supervision: M. Susan Lozier, Amy Bower, Stuart A. Cunningham, Brad deYoung, M. Femke de Jong, N. Penny Holliday, William E. Johns, Johannes Karstensen, Robert S. Pickart, Fiammetta Straneo
Visualization: Yao Fu
Writing – original draft: Yao Fu, M. Susan Lozier
Writing – review & editing: Yao Fu, M. Susan Lozier, Amy Bower, Kristin Burmeister, Tiago Carrilho Biló, Frédéric Cyr, Stuart A. Cunningham, Brad deYoung, Ahmad Fehmi Dilmahamod, M. Femke de Jong, Nora Fried, N. Penny Holliday, Neil J. Fraser, William E. Johns, Feili Li, Johannes Karstensen, Robert S. Pickart, Fiammetta Straneo, Igor Yashayaev

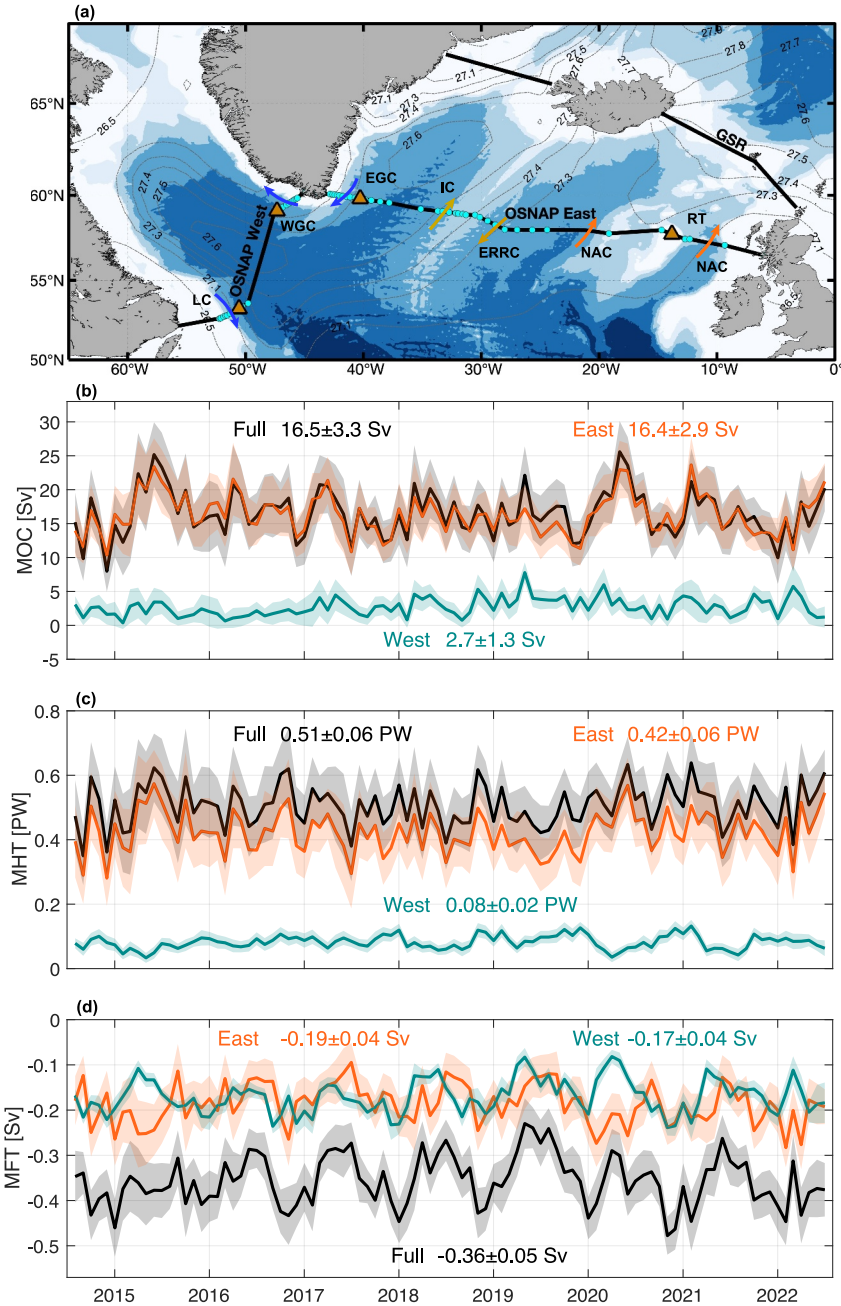

Figure 1. Map of the subpolar North Atlantic (a). Shading, indicating bathymetry at 500, 1,000, 2,000, and 3,000 m, is superimposed with the winter climatological sea surface potential density (σ_θ, kg m^{-3}) from EN4. Overturning in the Subpolar North Atlantic Program (OSNAP) West, OSNAP East, and Greenland-Scotland-Ridge (GSR) sections are indicated by thick black lines. OSNAP mooring positions are marked by cyan dots. Orange triangles mark the offshore extent of boundary current regions: Rockall Trough, East Greenland Current (EGC), West Greenland Current (WGC) and Labrador Current (LC). Arrows illustrate horizonal currents: North Atlantic Current, East Reykjanes Ridge Current, Irminger Current, EGC, WGC, and LC. Monthly time series for (b) the Meridional Overturning Circulation, (c) meridional heat transport, and (d) meridional freshwater transport across the full OSNAP array (black), OSNAP East (orange), and OSNAP West (cyan). Shading represents monthly uncertainty estimated using a Monte Carlo approach (Lozier et al., 2019).

Boundary currents play a key role in MOC dynamics because they are the main conduit for advecting waters throughout the SPNA and because during their transit they strongly interact with newly-convected waters in the basin interiors. Across the Iceland basin and the Rockall Trough (RT), the North Atlantic Current (NAC) transports warm and saline waters into the eastern SPNA with multiple branches, primarily residing in the MOC's

upper limb (σ_θ <27.55 kg m^{-3}). After circulating through the Iceland and Irminger basins, the waters, now cooled, freshened and densified, exit the eastern SPNA via the East Greenland Current (EGC) and enter the Labrador Sea via the West Greenland Current (WGC). The waters, further cooled and freshened as they transit this basin, exit via the Labrador Current (LC) and Deep Western Boundary Current (DWBC).

The Overturning in the Subpolar North Atlantic Program (OSNAP) array has continuously measured the subpolar MOC and meridional heat and freshwater transports (MHT and MFT, respectively) since 2014. The OSNAP West and East sections measure the overturning in the Labrador Sea and the eastern subpolar basin (the Irminger and Iceland basins and RT), respectively. The initial 2 years of OSNAP observations revealed that overturning in the eastern subpolar basin dominates the mean and variability of the total subpolar MOC, with a smaller contribution from the Labrador Sea (Lozier et al., 2019). Using 4 years of OSNAP data (2014–2018), Li et al. (2021) found that no individual boundary current accounted for more than 10% of the total MOC variability, contrasting with the traditional view that the western boundary current is a major contributor to MOC variability. Subsequent studies found that the EGC and the Irminger Sea interior flow together explained up to 55% of OSNAP East MOC variability on intraseasonal timescales, with the interior flow variability primarily driven by large-scale wind forcing (Li et al., 2024; Sanchez-Franks et al., 2024). An analysis of the OVIDE section (between Greenland and Portugal) attribtues MOC seasonal variability to density changes at the EGC (Mercier et al., 2024). However, the contributions of boundary and interior currents to the observed subpolar MOC variability on interannual timescales remains unexplored.

Surface-forced water mass transformation (SFWMT) is a key process converting light upper limb waters to dense lower limb waters. Consequently, the strength and variability of the overturning are expected to be linked to SFWMT (Josey et al., 2009; Marsh, 2000). Studies on the time-mean relationship between the MOC and SFWMT in the SPNA (Buckley et al., 2023; Evans et al., 2023; Petit et al., 2020) found that SFWMT explains the majority of the mean MOC strength, with diapycnal mixing playing an important but secondary role (Evans et al., 2023; Fu et al., 2024). For instance, in the Labrador Basin, mixing accounts for the formation of 36% of waters in the lower limb (Zou et al., 2024). The gradual freshening of saline Atlantic water circulating around the SPNA is also attributed to mixing with fresh coastal waters of Arctic origin and glacier melt (Bebieva & Lozier, 2023; Evans et al., 2023).

Prior to OSNAP, past studies investigating the time-varying SPNA MOC-SFWMT relationship included those using model data (Grist et al., 2012, 2014; Josey et al., 2009) and those using observations, where estimates of geostrophic thermal-wind currents were used to calculate the MOC (Desbruyères et al., 2019). For the latter study, SFWMT variability north of 45°N was found to lead MOC variability at 45°N by ∼5 years on interannual to decadal timescales. In the eastern SPNA, Petit et al. (2020) used the first 2-year OSNAP data to show a strong zero-lag relationship between SFWMT and volume gain in the lower limb, followed by a MOC peak in 5 months. Using a longer period provided by ocean reanlayses, Fu et al. (2024) found significant correlation between SFWMT and MOC interannual variability ($r = 0.46$ to 0.6. Unless stated otherwise, all correlation coefficients are significant at the 95% significance level.), with SFWMT leading by ∼1 year. With the 6-year OSNAP time series, Fu et al. (2023) investigated the seasonality of the subpolar MOC and attributed the MOC spring peak to winter SFWMT. These studies underscore the role of SFWMT in driving MOC variability across different timescales. However, a quantitative investigation of this relationship on interannual timescales using direct MOC observations is still lacking. In this study, we present the August 2014 to July 2022 OSNAP MOC, MHT and MFT time series (Section 2.1). Using this 8-year time series, we examine the relationship between MOC and boundary current variability on interannual timescales (Section 2.2.1). We then analyze the role of SFWMT in subpolar MOC interannual variability through a lower limb volume budget analysis (Section 2.2.2). Together, these analyses aim to improve our understanding of the characteristics and mechanisms of the subpolar MOC interannual variability.

2. Results

2.1. MOC, MHT and MFT Time Series

Over the 8-year period, the mean MOC strength across the full OSNAP array is 16.5 ± 3.3 Sv (0.5 Sv) (Note: For all reported values in this section, the standard deviation follows the mean and the standard error is in parentheses). Consistent with previous studies (Fu et al., 2023; Li et al., 2021; Lozier et al., 2019), overturning across OSNAP East (16.4 ± 2.9 Sv (0.5 Sv)) dominates the mean and variability of the total subpolar MOC (Figure 1b),

as indicated by the high correlation between the two time series ($r = 0.90$), while overturning across OSNAP West (2.7 ± 1.3 Sv (0.3 Sv)) plays a secondary role, with a lower correlation to the total MOC ($r = 0.45$). Please see Supporting Information S1 for MOC definiation and refer to Lozier et al. (2019) for the calculation details of the MOC, MHT and MFT.

The mean MHT across the full OSNAP array is 0.51 ± 0.06 PW (0.01 PW) (1 PW = 1×10^{15} W), with OSNAP East contributing 0.42 ± 0.06 PW (0.01 PW) and OSNAP West contributing 0.08 ± 0.02 PW (0.01 PW). Similar to the MOC, MHT variability across the full array is dominated by OSNAP East ($r = 0.95$), with much weaker variability at OSNAP West ($r = 0.18$) (Figure 1c).

MFT across the full OSNAP array has a mean of -0.36 ± 0.05 Sv (0.01 Sv) ("−" denotes southward MFT). MFT across OSNAP East and OSNAP West contribute -0.19 ± 0.04 Sv (0.01 Sv) and -0.17 ± 0.04 Sv (0.01 Sv) to this total, respectively. As reported previously, MFT across OSNAP East and OSNAP West contribute almost equally to the mean and variability of the total MFT (Figure 1d) (Lozier et al., 2019). See Table S1 in Supporting Information S1 for a compilation of the statistics noted in this section.

2.2. MOC Interannual Variability

The extended 8-year time series allows a more robust characterization of subpolar MOC seasonality identified by Fu et al. (2023) with reduced uncertainty (Figure S1 and Table S2 in Supporting Information S1). After removing seasonality from the MOC time series, we first investigate the relationship between MOC and boundary current interannual variability to explore whether a single boundary current can capture a larger portion of MOC variability than that reported by Li et al. (2021). We then focus on understanding MOC interannual variability due to surface buoyancy forcing, which transforms light upper-limb waters to dense lower-limb waters. The first part of our analysis is designed to understand the spatial components of the observed interannual variability, and the second part is designed to understand the mechanistic components of that variability.

2.2.1. Connection Between MOC and Boundary Current Variability

An interest in designing a cost-effective observing system, has led to the question as to whether a measure of eastern and western boundary transport is sufficient to capture the total MOC variability. For this exploration, we calculate the MOC using Supporting Information S1; Equation 1, in which time-varying density and velocity fields are used for part of the section and time mean values for the remainder of the section. For the calculation from east to west, the fields to the east of each grid point are time-varying and the fields to the west are constant. A parallel calculation is done from west to east, where the fields to the west (east) of each grid point are time-varying (constant). This calculation reveals the cumulative contribution of different parts of the basin to the total MOC variance, and it allows the contributions of key boundary currents to be isolated. For each calculation of the explained MOC variance, we use (a) the unfiltered monthly time series and (b) the deseasonalized and 1-year lowpass filtered time series (12-month Butterworth filter) to examine the explained MOC variance on interannual timescales (see Supporting Information S1 for additional details). With this analysis, we acknowledge that the eastern boundary current across OSNAP East is not easily defined and so we adopt a stepwise approach: we first consider the flow through the RT as the eastern boundary and then move westward from there, increasingly capturing the myriad currents that comprise the NAC.

Accumulating from east to west (Figure 2a), the explained MOC variance across the eastern subpolar basin rapidly increases as the northward NAC branches in the RT and Iceland Basin are included. It reaches between 73% and 84% at the Reykjanes Ridge (hereafter RR; at ~31°W) for both the unfiltered and filtered time series. Likewise, accumulating from west to east (Figure 2b), the explained MOC variance sharply increases to 73% (82%) using the unfiltered (filtered) time series between East Greenland and 31°W. When only a single boundary current is considered, the explained MOC variance across OSNAP East is much reduced: using the unfiltered time series, RT explains 19% of the MOC variance and the EGC explains 22% (Figure S2 and Table S3 in Supporting Information S1), nearly doubling the values estimated by Li et al. (2021) for the shorter time series. On interannual timescales (Figure 2c), the explained variance increases to 36% and 39% for the RT and EGC, respectively. We purposely select these narrowly confined regions at the boundaries to examine their capability to capture MOC interannual variability. Including all NAC branches (i.e., from 26°W to the Scottish Shelf), the explained MOC variance rises to 49% and 69% for the original and filtered time series, respectively. Given the strong (east to west) upward slope of $\overline{\sigma_{MOCE}}$, the MOC upper limb is contained largely in the area between the Scottish shelf and

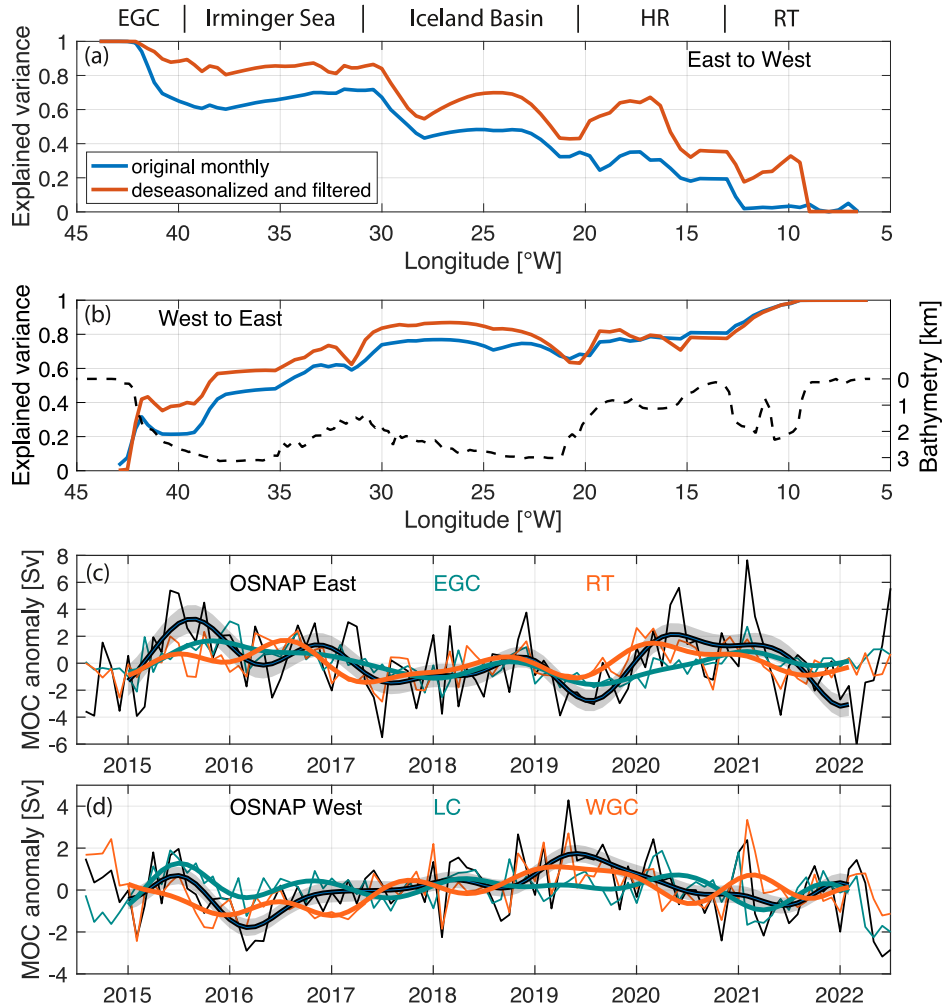

Figure 2. Overturning variability represented by boundary currents and the basin interior. Overturning in the Subpolar North Atlantic Program (OSNAP) East Meridional Overturning Circulation (MOC) variance explained by accumulated transport variability (a) from east to west and (b) from west to east by using the unfiltered (blue) and filtered (red; see Supporting Information S1 Methods) time series. Geographic locations are marked along the top of (a). HR represents the Hatton-Rockall Basin. Note that East Greenland Current (EGC) is part of the Irminger Sea. Bathymetry is shown as black-dashed line in (b). (c) MOC anomalies derived from OSNAP East (black), time-varying EGC (green), and time-varying Rockall Trough (orange). (d) MOC anomalies derived from OSNAP West (black), time-varying Labrador Current (green), and time-varying West Greenland Current (orange). The thin (thick) lines in (c) and (d) represent the deseasonalized (1-year Butterworth lowpass filtered) time series. All time series are detrended. The uncertainty of the MOC anomaly time series (shading) is calculated as the standard deviation of realizations of the filtered MOC anomaly time series derived from Monte Carlo methods (Lozier et al., 2019).

RR, while the lower limb lies between East Greenland and RR. Our results indicate that overall MOC interannual variability can be equally characterized by capturing the warm, saline upper-limb waters east of RR, or the cooled, freshened lower-limb waters west of RR.

We next turn to the western subpolar basin, where the two boundary currents (WGC and LC including their deeper extensions) dominate MOC variability. When LC and WGC are combined, that is, using time-varying velocity and density in both currents and climatology in between, the explained MOC variance reaches 81% and 87% using the unfiltered and filtered time series, respectively. However, using the unfiltered time series, the WGC alone explains only 14% of OSNAP West MOC variance and the LC alone accounts for 7%, both similar to the previous estimate (~10%) by Li et al. (2021) using a shorter time series. On interannual timescales, the WGC and LC account for 42% and 25% of the OSNAP West MOC variance, respectively (Figure 2d and Table S3 in Supporting Information S1). Overall, the analysis suggests that individual boundary currents account for a greater portion of

OSNAP West MOC variance when shorter-term variability (seasonal and shorter) is removed. However, regardless of timescale, variability in both WGC and LC is needed to explain the bulk of MOC variance and the interior flow contributes only a small fraction in this basin (Figure S3 in Supporting Information S1).

2.2.2. Lower Limb Volume Budget

We next examine MOC interannual variability through the framework of a volume budget for the lower limb by considering volume change ($\frac{dVol}{dt}$), SFWMT, export ($-E$), and residual (R) for the period of August 2014 to July 2022:

$$\frac{dVol}{dt}(t) = \mathrm{SFWMT}(t) - E(t) + R(t) \tag{1}$$

where $R(t)$ is understood to include unresolved processes contributing to lower limb volume change, such as water mass transformation due to mixing and wind-driven transformation (e.g., due to Ekman buoyancy fluxes; Le Bras et al., 2022) as well as any measurement errors. We analyze the budgets for the western and eastern basins, separately, using the time-mean $\overline{\sigma_{\mathrm{MOC}}}$ of each basin as the isopycnal separating the upper and lower limbs. $\frac{dVol}{dt}$ is calculated by determining the change of layer thickness between $\overline{\sigma_{\mathrm{MOC}}}$ and the seafloor from three density fields: Met Office EN4.2.2 (Good et al., 2013), monthly Argo climatology (Roemmich & Gilson, 2009), and ARMOR3D (Guinehut et al., 2012; Mulet et al., 2012). SFWMT is calculated following Petit et al. (2020) by using each of the density products listed above with each of the surface heat and freshwater fluxes from ERA5 atmospheric reanalysis (Poli et al., 2016) and NCEP Climate Forecast System Version 2 (Saha et al., 2014). The mean of the 6 combinations is used for the volume budget. E for the eastern basin is the difference between the incoming overflow waters across the Greenland-Scotland Ridge (GSR) and the outgoing deep waters below $\overline{\sigma_{\mathrm{MOC}E}}$ across OSNAP East, which is estimated using OSNAP and GSR (Bringedal et al., 2018) transport measurements. E for the western basin is the transport below $\overline{\sigma_{\mathrm{MOC}W}}$ across OSNAP West (See Supporting Information S1 for detail). We note that deep waters are formed in both the interior and boundary regions, but they are primarily exported by boundary currents. In the volume budget, E is an integrated measure of the total transport of water out of the basins without distinguishing between the boundary and interior. We first examine how well the lower limb volume budget can be closed in the mean, followed by an analysis of the time-varying relationships among the budget terms.

The mean volume change, $\overline{\frac{dVol}{dt}}$ is close to 0 for both eastern and western subpolar basins (<0.2 Sv). The residual, $\overline{R}$, primarily determined by $-\left(\overline{\mathrm{SFWMT}} - \overline{E}\right)$, serves as a measure of the unresolved processes, such as mixing, required to close the mean volume budget. In the eastern subpolar basin, $\overline{\mathrm{SFWMT}}$ and $-\overline{E}$ are 4.1 ± 0.4 Sv and −6.4 ± 0.5 Sv, respectively, resulting in a residual of 2.3 ± 0.4 Sv. In the western subpolar basin, $\overline{\mathrm{SFWMT}}$ and $-\overline{E}$ are 1.7 ± 0.3 Sv and −3.3 ± 0.2 Sv, respectively, resulting in a residual of 1.6 ± 0.4 Sv. The mean residual in the western subpolar basin is relatively large with respect to the mean OSNAP West MOC (2.7 ± 0.3 Sv), whereas in the eastern subpolar basin the residual accounts for a smaller portion of the mean OSNAP East MOC (16.4 ± 0.5 Sv).

Together, these findings indicate that the mean lower limb volume budget can be closed within about 2 Sv for the subpolar basins using independent data sets. They also suggest that unresolved processes such as mixing-induced transformation plays a more active role proportionally in the western subpolar basin compared to the eastern subpolar basin. Previous studies have reported that ∼6 Sv of overflow waters are formed through entrainment after crossing the GSR (Hansen et al., 2016; Jochumsen et al., 2015; Johns et al., 2021), larger than the mixing-induced transformation inferred here for the eastern subpolar basin. This difference indicates that most of the entrainment adds to waters already within the lower limb.

Next, we investigate the zero-lag relationships among the volume budget terms based on the deseasonalized and 1-year lowpass filtered time series (Figure 3). $\frac{dVol}{dt}(t)$ is well correlated with the sum of SFWMT and export (i.e., $\mathrm{SFWMT}(t) - E(t)$) in both the eastern and western subpolar basins ($r = 0.71$ and $r = 0.80$, respectively). This correlation is primarily driven by the strong relationship between $\frac{dVol}{dt}(t)$ and $\mathrm{SFWMT}(t)$ at zero lag, with $r = 0.89$ in the eastern subpolar basin and $r = 0.69$ in the western subpolar basin (Figures S4a and S4b in

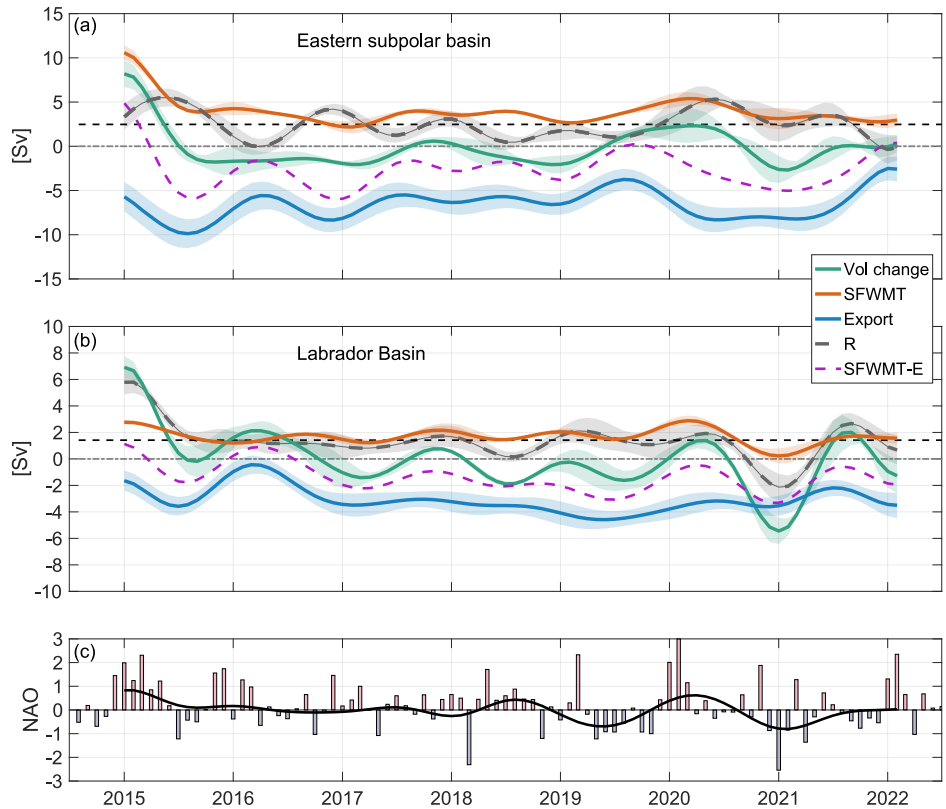

Figure 3. Time series of volume change (green), Surface-forced water mass transformation (SFWMT) (red), export (-E, blue), residual (R, thick black dashed) and the sum of SFWMT and export (magenta dashed) for (a) the eastern subpolar basin, and (b) the western subpolar basin. Thin black dashed line indicates the time mean residual. Shading represents uncertainty calculated as explained in SI Methods. Time series in (a) and (b) are deseasonalized and 1-year lowpass filtered. (c) Hurrell-monthly North Atlantic Oscillation index (bar) with 1-year lowpass filtered time series overlaid (black line).

Supporting Information S1). In contrast, $\frac{dVol}{dt}(t)$ is not significantly correlated with export at zero lag (Figures S4c and S4d in Supporting Information S1).

We now investigate the lead-lag relationships among SFWMT, volume change, and export. In the eastern subpolar basin (Figure 3a and Figure S4 in Supporting Information S1), the maximum negative correlation between SFWMT and export ($r = -0.62$) and between volume change and export ($r = -0.58$) occurs when SFWMT and volume change lead export by about 6 months, consistent with the findings of Petit et al. (2020) using the shorter time series. For example, stronger SFWMT and volume change in 2015 are followed by enhanced export/MOC in a few months. Together with the relationships found at zero lag, the lead-lag relationships suggest that dense water formation through surface buoyancy fluxes immediately increases the lower limb volume, subsequently leading to enhanced export/MOC within a year.

In the western subpolar basin (Figure 3b and Figure S4 in Supporting Information S1), the maximum correlation between SFWMT and export ($r = 0.52$) occurs when SFWMT leads by 4 months, and volume change does not exhibit a significant correlation with export at any lag less than 1 year. The difference between OSNAP East and West may be due to 1) the larger proportional contribution of diapycnal mixing to the total water mass transformation at OSNAP West (Zou et al., 2024), which complicates the relationship between volume change and export; and/or 2) a lower signal-to-noise ratio for OSNAP West given its relatively small export compared to OSNAP East.

3. Discussion and Conclusions

Using the 8-year OSNAP time series, we investigate MOC interannual variability and the extent to which it can be captured by boundary current variability. We find that variability in any single boundary current can account for a

modest portion (~30%) of MOC variance. Instead, a comparison of east-to-west and west-to-east cumulative explained variance along OSNAP East demonstrates that the entire upper or lower limb is needed to capture a significant portion of the total MOC variance, in agreement with previous studies highlighting the importance of the Irminger Sea for MOC variance (Chafik et al., 2022; Sanchez-Franks et al., 2024). In contrast, MOC interannual variability at OSNAP West is predominantly reproduced by the combined LC and WGC variability. By highlighting regions that contribute significantly to MOC interannual variability, these results could be used to design a more cost-efficient OSNAP configuration.

Through a volume budget analysis, we found the expected relationships in the eastern subpolar basin, that is, strengthened SFWMT increases lower limb volume, leading to an enhanced MOC in the same year. Variability in SFWMT explains ~38% of MOC variance ($r = 0.62$) with SFWMT leading by 6 months. The short time lag between SFWMT and export may reflect the fact that SFWMT variability at densities close to $\overline{\sigma_{MOC}}$ is primarily observed along the subpolar gyre pathway (i.e., boundaries and RR) (Petit et al., 2021), leading to a rapid export of the newly formed dense water from the subpolar basins (Fu et al., 2023; Koelling et al., 2022; Le Bras et al., 2020). However, the existence of different pathways and timescales for the waters in the basin (Tooth et al., 2023) implies that the composition of the exported water is likely a mixture of newly formed and preexisting waters, such that the lag cannot be associated with a single pathway. In the western subpolar basin, although SFMWT is significantly correlated with the MOC ($r = 0.52$), we do not detect a linkage between volume change and MOC on interannual timescales.

We also found a difference between OSNAP East and West in their relationship with North Atlantic Oscillation (NAO) (Figure 3c): OSNAP East MOC has a maximum correlation with NAO ($r = 0.56$) on interannual timescales with NAO leading by 4 months, while OSNAP West MOC is not significantly correlated with the NAO. Notably, the winter in 2015 is characterized by a strongly positive NAO, which is typically associated with enhanced sea surface heat loss, higher precipitation, and higher production of dense water in the SPNA (de Jong & de Steur, 2016; Yashayaev, 2024). Though the NAO-MOC correlation found at OSNAP East is modest, the correlation may be stronger on longer timescales or for other periods, as indicated by modeling studies focusing on lower latitudes (Danabasoglu et al., 2012; Oldenburg et al., 2021; Sun et al., 2021).

The unprecedented freshening in the eastern SPNA since 2012 (Holliday et al., 2020) was followed by a freshening of the Labrador Sea since 2022 (Yashayaev, 2024). The impact of this freshening on deep convection and circulation have been documented in both the Irminger Sea (Biló et al., 2022; Fried et al., 2024) and the Labrador Sea (Yashayaev, 2024). Furthermore, Koman et al. (2024) reported a freshening-induced thinning of the DWBC layer off East Greenland that resulted in a 26% weakening of the DWBC transport from 2014 to 2020. Despite these substantial changes, no weakening trend in the MOC across the full OSNAP array is evident from the 8-year record.

As a possible explanation, we note that the overturning at OSNAP East and OSNAP West are anti-correlated on interannual timescales (Figures 2c and 2d), with a maximum correlation of −0.64 when OSNAP East overturning leads by a few months. We suggest that overturning variability in the eastern and western subpolar basins may partially offset each other. Furthermore, the persistently positive NAO since 2012 has produced high-density anomalies in the SPNA through excessive cooling, which may offset the low-density anomalies associated with the freshening. Together, these processes may contribute to the relative stability of the MOC across the entire SPNA. The mechanisms underlying the west-east anti-correlation remain unclear and motivate further investigation with a longer time series.

Moving forward, a major concern is the potential shift in the Beaufort gyre (Lin et al., 2023), which has accumulated an enormous reservoir of freshwater over the past decades. A key question facing the MOC community is the impact on subpolar MOC and MFT if/when this freshwater is released into the SPNA. Future analyses of the OSNAP time series will focus on the relationship between subpolar freshening and the MOC in the hope that we can shed some light on this impact. Finally, we will continue to explore the impact of MOC variability on the MHT given the strong link between the two.

Data Availability Statement

The 2014–2022 OSNAP data are available via Fu et al. (2025). The ECMWF ERA5 data are available via Hersbach et al. (2023). The NCEP surface heat and freshwater fluxes are available via Saha et al. (2012). The Met Office EN4.2.2.g10 data are available via Good et al. (2013). The DSOW transport is available via Jochumsen et al. (2017a, 2017b). The FBC transport is available via Larsen et al. (2024a, 2024b). ARMOR3D data are available via Copernicus (2012).

Acknowledgments

OSNAP data were collected and made freely available by the Overturning in the Subpolar North Atlantic Program and all the national programs that contribute to it (www.o-snap.org). The OSNAP moorings are part of the OceanSITES coordination network of the GOOS. We acknowledge funding from the Physical Oceanography Program of the U.S. National Science Foundation (OCE-1259398, OCE-1756231, OCE-1948335, OCE-1948482, OCE-1259618, OCE-1756363, OCE-1756361, OCE-1948505, OCE-1948198); F.D. and J.K. acknowledge funding from EU Horizon Europe programmes under Grant agreement No.101136548 (ObsSea4Clim) and No.862626 (EuroSea). The Dutch OSNAP contribution is financially supported by the Innovational Research Incentives Scheme of the Netherlands Organisation for Scientific Research (NWO) under Grant agreement nos.016.Vidi.189.130 and NIOZ-Utrecht University grant "The impact of atmospheric noise on the Atlantic Meridional Overturning Circulation." The UK OSNAP contribution was supported by the UK Natural Environment Research Council (NERC) National Capability programme AtlantiS (NE/Y005589/1), NERC grants UK-OSNAP (NE/K010875/2), and UK-OSNAP-Decade (NE/T00858X/1). F.L. acknowledges support from the National Key R&D Program of China (2023YFF0805102). The Canadian OSNAP contribution is supported by the Atlantic Zone Monitoring Program of Fisheries and Oceans Canada. We also thank Sam Jones, Lewis Drysdale, and Estelle Dumont for their helpful comments on the manuscript.

References

Årthun, M., Asbjørnsen, H., Chafik, L., Johnson, H. L., & Våge, K. (2023). Future strengthening of the Nordic Seas overturning circulation. *Nature Communications*, *14*(1), 2065. https://doi.org/10.1038/s41467-023-37846-6

Bebieva, Y., & Lozier, M. S. (2023). Fresh water and atmospheric cooling control on density-compensated overturning in the Labrador Sea. *Journal of Physical Oceanography*, *53*(11), 2575–2589. https://doi.org/10.1175/JPO-D-22-0238.1

Biló, T. C., Straneo, F., Holte, J., & Le Bras, I. A. A. (2022). Arrival of new great salinity anomaly weakens convection in the Irminger Sea. *Geophysical Research Letters*, *49*(11), 1–10. https://doi.org/10.1029/2022GL098857

Bringedal, C., Eldevik, T., Skagseth, Ø., Spall, M. A., & Østerhus, S. (2018). Structure and forcing of observed exchanges across the Greenland-Scotland ridge. *Journal of Climate*, *31*(24), 9881–9901. https://doi.org/10.1175/JCLI-D-17-0889.1

Buckley, M. W., Lozier, M. S., Desbruyères, D., & Evans, D. G. (2023). Buoyancy forcing and the subpolar Atlantic meridional overturning circulation. *Philosophical Transactions of the Royal Society A: Mathematical, Physical and Engineering Sciences*, *381*(2262). https://doi.org/10.1098/rsta.2022.0181

Chafik, L., Holliday, N. P., Bacon, S., & Rossby, T. (2022). Irminger sea is the center of action for subpolar AMOC variability. *Geophysical Research Letters*, *49*(17), e2022GL099133. https://doi.org/10.1029/2022GL099133

Collins, M., Sutherland, M., Bouwer, L., Cheong, S.-M., Frölicher, T. L., Jacot Des Combes, H., et al. (2019). Extremes, abrupt changes and managing risks. *IPCC Special Report on the Ocean and Cryosphere in a Changing Climate*, 589–655. Retrieved from https://report.ipcc.ch/srocc/pdf/SROCC_FinalDraft_Chapter6.pdf

Copernicus. (2012). Multi observation global Ocean 3D temperature salinity height geostrophic current and MLD [Dataset]. *Copernicus Marine Service*. https://doi.org/10.48670/moi-00052

Danabasoglu, G., Yeager, S. G., Kwon, Y.-O., Tribbia, J. J., Phillips, A. S., & Hurrell, J. W. (2012). Variability of the Atlantic meridional overturning circulation in CCSM4. *Journal of Climate*, *25*(15), 5153–5172. https://doi.org/10.1175/JCLI-D-11-00463.1

de Jong, M. F., & de Steur, L. (2016). Strong winter cooling over the Irminger Sea in winter 2014–2015, exceptional deep convection, and the emergence of anomalously low SST. *Geophysical Research Letters*, *43*(13), 7106–7113. https://doi.org/10.1002/2016GL069596

Desbruyères, D. G., Mercier, H., Maze, G., & Daniault, N. (2019). Surface predictor of overturning circulation and heat content change in the subpolar North Atlantic. *Ocean Science*, *15*(3), 809–817. https://doi.org/10.5194/os-15-809-2019

Evans, D. G., Holliday, N. P., Bacon, S., & Le Bras, I. (2023). Mixing and air-sea buoyancy fluxes set the time-mean overturning circulation in the subpolar North Atlantic and Nordic Seas. *Ocean Science*, *19*(3), 745–768. https://doi.org/10.5194/os-19-745-2023

Fried, N., Biló, T. C., Johns, W. E., Katsman, C. A., Fogaren, K. E., Yoder, M., et al. (2024). Recent freshening of the subpolar North Atlantic increased the transport of lighter waters of the Irminger current from 2014 to 2022. *Journal of Geophysical Research: Oceans*, *129*(11), e2024JC021184. https://doi.org/10.1029/2024JC021184

Fu, Y., Lozier, M. S., Biló, T. C., Bower, A. S., Cunningham, S. A., Cyr, F., et al. (2023). Seasonality of the meridional overturning circulation in the subpolar North Atlantic. *Communications Earth & Environment*, *4*(1), 181. https://doi.org/10.1038/s43247-023-00848-9

Fu, Y., Lozier, M. S., Bower, A. S., Burmeister, K., Biló, T. C., Cyr, F., et al. (2025). Meridional overturning circulation observed by the overturning in the subpolar North Atlantic program (OSNAP) array from August 2014 to July 2022 [Dataset]. *Georgia Tech Digital Repository*. https://doi.org/10.35090/gatech/78023

Fu, Y., Lozier, M. S., Majumder, S., & Petit, T. (2024). Water mass transformation and its relationship with the overturning circulation in the Eastern subpolar North Atlantic. *Journal of Geophysical Research: Oceans*, *129*(12), e2024JC021222. https://doi.org/10.1029/2024JC021222

Good, S. A., Martin, M. J., & Rayner, N. A. (2013). EN4: Quality controlled ocean temperature and salinity profiles and monthly objective analyses with uncertainty estimates. *Journal of Geophysical Research: Oceans*, *118*(12), 6704–6716. https://doi.org/10.1002/2013JC009067

Grist, J. P., Josey, S. A., & Marsh, R. (2012). Surface estimates of the Atlantic overturning in density space in an eddy-permitting ocean model. *Journal of Geophysical Research*, *117*(6). https://doi.org/10.1029/2011JC007752

Grist, J. P., Josey, S. A., Marsh, R., Kwon, Y. O., Bingham, R. J., & Blaker, A. T. (2014). The surface-forced overturning of the North Atlantic: Estimates from modern era atmospheric reanalysis datasets. *Journal of Climate*, *27*(10), 3596–3618. https://doi.org/10.1175/JCLI-D-13-00070.1

Guinehut, S., Dhomps, A.-L., Larnicol, G., & Le Traon, P.-Y. (2012). High resolution 3-D temperature and salinity fields derived from in situ and satellite observations. *Ocean Science*, *8*(5), 845–857. https://doi.org/10.5194/os-8-845-2012

Hansen, B., Húsgarð Larsen, K. M., Hátún, H., & Østerhus, S. (2016). A stable faroe bank channel overflow 1995–2015. *Ocean Science*, *12*(6), 1205–1220. https://doi.org/10.5194/os-12-1205-2016

Hersbach, H., Bell, B., Berrisford, P., Biavati, G., Horányi, A., Muñoz Sabater, J., et al. (2023). ERA5 monthly averaged data on single levels from 1940 to present [Dataset]. *Copernicus Climate Change Service (C3S) Climate Data Store (CDS)*. https://doi.org/10.24381/cds.f17050d7

Holliday, N. P., Bersch, M., Berx, B., Chafik, L., Cunningham, S., Florindo-López, C., et al. (2020). Ocean circulation causes the largest freshening event for 120 years in eastern subpolar North Atlantic. *Nature Communications*, *11*(1), 585. https://doi.org/10.1038/s41467-020-14474-y

Jochumsen, K., Moritz, M., Nunes, N., Quadfasel, D., Larsen, K. M. H., Hansen, B., et al. (2017b). Overflow time-series through Denmark Strait [Dataset]. *Integrated Climate Data Center (ICDC)*. https://www.cen.uni-hamburg.de/en/icdc/data/ocean/denmark-strait-overflow.html

Jochumsen, K., Köllner, M., Quadfasel, D., Dye, S., Rudels, B., & Valdimarsson, H. (2015). On the origin and propagation of Denmark Strait overflow water anomalies in the Irminger Basin. *Journal of Geophysical Research: Oceans*, *120*(3), 1841–1855. https://doi.org/10.1002/2014JC010397

Jochumsen, K., Moritz, M., Nunes, N., Quadfasel, D., Larsen, K. M. H., Hansen, B., et al. (2017a). Revised transport estimates of the Denmark Strait overflow. *Journal of Geophysical Research: Oceans*, *122*(4), 3434–3450. https://doi.org/10.1002/2017JC012803

Johns, W. E., Devana, M., Houk, A., & Zou, S. (2021). Moored observations of the Iceland-Scotland overflow plume along the Eastern flank of the Reykjanes ridge. *Journal of Geophysical Research: Oceans*, *126*(8), 1–26. https://doi.org/10.1029/2021JC017524

Josey, S. A., Grist, J. P., & Marsh, R. (2009). Estimates of meridional overturning circulation variability in the North Atlantic from surface density flux fields. *Journal of Geophysical Research*, *114*(9). https://doi.org/10.1029/2008JC005230

Koelling, J., Atamanchuk, D., Karstensen, J., Handmann, P., & Wallace, D. W. R. (2022). Oxygen export to the deep ocean following labrador sea water formation. *Biogeosciences*, *19*(2), 437–454. https://doi.org/10.5194/bg-19-437-2022

Koman, G., Bower, A. S., Holliday, N. P., Furey, H. H., Fu, Y., & Biló, T. C. (2024). Observed decrease in Deep Western Boundary Current transport in subpolar North Atlantic. *Nature Geoscience*, *17*(11), 1148–1153. https://doi.org/10.1038/s41561-024-01555-6

Larsen, K. M. H., Hansen, B., Hátún, H., Johansen, G. E., Østerhus, S., & Olsen, S. M. (2024b). Time series of FBC overflow transport, FBC bottom temperature and Atlantic water properties [Dataset]. *Environmental data on terrestrial and marine ecosystems in the Faroe Islands (ENVOFAR)*. https://envofar.fo/data/index.php?dir=Timeseries&sort=N&order=A

Larsen, K. M. H., Hansen, B., Hátún, H., Johansen, G. E., Østerhus, S., & Olsen, S. M. (2024a). The coldest and densest overflow branch into the North Atlantic is stable in transport, but warming. *Geophysical Research Letters*, *51*(16), e2024GL110097. https://doi.org/10.1029/2024GL110097

Le Bras, I. A.-A., Callies, J., Straneo, F., Biló, T. C., Holte, J., & Johnson, H. L. (2022). Slantwise convection in the Irminger Sea. *Journal of Geophysical Research: Oceans*, *127*(10), e2022JC019071. https://doi.org/10.1029/2022JC019071

Le Bras, I. A. A., Straneo, F., Holte, J., de Jong, M. F., & Holliday, N. P. (2020). Rapid export of waters formed by convection near the Irminger Sea's Western boundary. *Geophysical Research Letters*, *47*(3), e2019GL085989. https://doi.org/10.1029/2019GL085989

Li, F., Fu, Y., Lozier, M. S., Le Bras, I. A., de Jong, M. F., Wang, Y., & Sanchez-Franks, A. (2024). Deep circulation variability through the eastern subpolar North Atlantic. *Journal of Climate*, *37*(23), 6221–6234. https://doi.org/10.1175/jcli-d-23-0487.1

Li, F., Lozier, M. S., Bacon, S., Bower, A. S., Cunningham, S. A., de Jong, M. F., et al. (2021). Subpolar North Atlantic western boundary density anomalies and the meridional overturning circulation. *Nature Communications*, *12*(1), 1–9. https://doi.org/10.1038/s41467-021-23350-2

Lin, P., Pickart, R. S., Heorton, H., Tsamados, M., Itoh, M., & Kikuchi, T. (2023). Recent state transition of the Arctic Ocean's beaufort gyre. *Nature Geoscience*, *16*(6), 485–491. https://doi.org/10.1038/s41561-023-01184-5

Lozier, M. S., Li, F., Bacon, S., Bahr, F., Bower, A. S., Cunningham, S. A., et al. (2019). A sea change in our view of overturning in the subpolar North Atlantic. *Science*, *363*(6426), 516–521. https://doi.org/10.1126/science.aau6592

Marsh, R. (2000). Recent variability of the north Atlantic thermohaline circulation inferred from surface heat and freshwater fluxes. *Journal of Climate*, *13*(18), 3239–3260. https://doi.org/10.1175/1520-0442(2000)013<3239:RVOTNA>2.0.CO;2

Mercier, H., Desbruyères, D., Lherminier, P., Velo, A., Carracedo, L., Fontela, M., & Pérez, F. F. (2024). New insights into the eastern subpolar North Atlantic meridional overturning circulation from OVIDE. *Ocean Science*, *20*(3), 779–797. https://doi.org/10.5194/os-20-779-2024

Mulet, S., Rio, M.-H., Mignot, A., Guinehut, S., & Morrow, R. (2012). A new estimate of the global 3D geostrophic ocean circulation based on satellite data and in-situ measurements. *Deep Sea Research Part II: Topical Studies in Oceanography*, *77–80*, 70–81. https://doi.org/10.1016/j.dsr2.2012.04.012

Oldenburg, D., Wills, R. C. J., Armour, K. C., Thompson, L., & Jackson, L. C. (2021). Mechanisms of low-frequency variability in north atlantic ocean heat transport and AMOC. *Journal of Climate*, *34*(12), 4733–4755. https://doi.org/10.1175/JCLI-D-20-0614.1

Petit, T., Lozier, M. S., Josey, S. A., & Cunningham, S. A. (2020). Atlantic deep water formation occurs primarily in the Iceland basin and Irminger Sea by local buoyancy forcing. *Geophysical Research Letters*, *47*(22), 1–9. https://doi.org/10.1029/2020GL091028

Petit, T., Lozier, M. S., Josey, S. A., & Cunningham, S. A. (2021). Role of air-sea fluxes and ocean surface density in the production of deep waters in the eastern subpolar gyre of the North Atlantic. *Ocean Science*, *17*(5), 1353–1365. https://doi.org/10.5194/os-17-1353-2021

Poli, P., Hersbach, H., Dee, D. P., Berrisford, P., Simmons, A. J., Vitart, F., et al. (2016). ERA-20C: An atmospheric reanalysis of the twentieth century. *Journal of Climate*, *29*(11), 4083–4097. https://doi.org/10.1175/JCLI-D-15-0556.1

Roemmich, D., & Gilson, J. (2009). The 2004–2008 mean and annual cycle of temperature, salinity, and steric height in the global ocean from the argo program. *Progress in Oceanography*, *82*(2), 81–100. https://doi.org/10.1016/j.pocean.2009.03.004

Saha, S., Moorthi, S., Wu, X., Wang, J., Nadiga, S., Tripp, P., et al. (2012). NCEP Climate Forecast System Version 2 (CFSv2) monthly products [Dataset]. *NSF National Center for Atmospheric Research*. https://doi.org/10.5065/D69021ZF

Saha, S., Moorthi, S., Wu, X., Wang, J., Nadiga, S., Tripp, P., et al. (2014). The NCEP climate forecast system version 2. *Journal of Climate*, *27*(6), 2185–2208. https://doi.org/10.1175/JCLI-D-12-00823.1

Sanchez-Franks, A., Holliday, N. P., Evans, D. G., Fried, N., Tooth, O., Chafik, L., et al. (2024). The irminger gyre as a key driver of the subpolar North Atlantic overturning. *Geophysical Research Letters*, *51*(8), e2024GL108457. https://doi.org/10.1029/2024GL108457

Sun, C., Zhang, J., Li, X., Shi, C., Gong, Z., Ding, R., et al. (2021). Atlantic meridional overturning circulation reconstructions and instrumentally observed multidecadal climate variability: A comparison of indicators. *International Journal of Climatology*, *41*(1), 763–778. https://doi.org/10.1002/joc.6695

Tooth, O. J., Johnson, H. L., & Wilson, C. (2023). Lagrangian overturning pathways in the Eastern subpolar North Atlantic. *Journal of Climate*, *36*(3), 823–844. https://doi.org/10.1175/JCLI-D-21-0985.1

Weijer, W., Haine, T., Siddiqui, A., Cheng, W., Veneziani, M., & Kurtakoti, P. (2022). Interactions between the Arctic mediterranean and the Atlantic meridional overturning circulation: A review. *Oceanography*, *35*(3). https://doi.org/10.5670/oceanog.2022.130

Yashayaev, I. (2024). Intensification and shutdown of deep convection in the labrador sea were caused by changes in atmospheric and freshwater dynamics. *Communications Earth & Environment*, *5*(1), 156. https://doi.org/10.1038/s43247-024-01296-9

Zou, S., Petit, T., Li, F., & Lozier, M. S. (2024). Observation-based estimates of water mass transformation and Formation in the labrador sea. *Journal of Physical Oceanography*, *54*(7), 1411–1429. https://doi.org/10.1175/JPO-D-23-0235.1

References From the Supporting Information

Curry, B., Lee, C. M., Petrie, B., Moritz, R. E., & Kwok, R. (2014). Multiyear volume, liquid freshwater, and sea ice transports through Davis Strait, 2004–10. *Journal of Physical Oceanography*, *44*(4), 1244–1266. https://doi.org/10.1175/JPO-D-13-0177.1

Hansen, B., Margretha Húsgar Larsen, K., Malskær Olsen, S., Quadfasel, D., Jochumsen, K., & Østerhus, S. (2018). Overflow of cold water across the iceland-faroe ridge through the Western Valley. *Ocean Science*, *14*(4), 871–885. https://doi.org/10.5194/os-14-871-2018

Li, F., Lozier, M. S., & Johns, W. E. (2017). Calculating the meridional volume, heat, and freshwater transports from an observing System in the subpolar North Atlantic: Observing System simulation experiment. *Journal of Atmospheric and Oceanic Technology*, *34*(7), 1483–1500. https://doi.org/10.1175/JTECH-D-16-0247.1

Sherwin, T. J., Griffiths, C. R., Inall, M. E., & Turrell, W. R. (2008). Quantifying the overflow across the Wyville Thomson ridge into the rockall trough. *Deep-Sea Research Part I Oceanographic Research Papers*, *55*(4), 396–404. https://doi.org/10.1016/j.dsr.2007.12.006

Speer, K., & Tziperman, E. (1992). Rates of water mass formation in the North Atlantic Ocean. *Journal of Physical Oceanography*, *22*(1), 93–104. https://doi.org/10.1175/1520-0485(1992)022<0093:ROWMFI>2.0.CO;2